

## Vietnam Journal of Catalysis and Adsorption Tạp chí xúc tác và hấp phụ Việt Nam

http://chemeng.hust.edu.vn/jca/

# Synthesis of WO<sub>3</sub>/Ag<sub>3</sub>VO<sub>4</sub> photocatalyst with enhanced visible light efficiency photocatalysis

Nguyen Thi Phuong Le Chi<sup>1\*</sup>, Tran Thi Thu Phuong<sup>2</sup>, Do Minh The<sup>2</sup>, Nguyen Tri Quoc<sup>3</sup>, Nguyen Thi Thanh Binh<sup>2</sup>, Tran Thi Thu Hien<sup>2</sup>, Mai Hung Thanh Tung<sup>4</sup>, Nguyen Vu Ngoc Mai<sup>2</sup>, Phan Thi Dieu<sup>2</sup>, Nguyen Thi Dieu Cam<sup>2</sup>

<sup>1</sup>Hochiminh City University of Natural Resources and Environment, 236B Le Van Sy Street, Ward 1, Tan Binh District, Hochiminh City, Vietnam

#### ARTICLE INFO

## Received: 10/5/2022 Accepted: 10/7/2022 Published: 15/7/2022

### Keywords:

 $WO_3/Ag_3VO_4$ , photocatalyst; degradation, Amoxicillin, antibiotic pollutant, visible region

#### **ABSTRACT**

 $WO_3/Ag_3VO_4$  photocatalyst was synthesized for benefiting the visible region of solar spectrum for degradation of antibiotic pollutant. The prepared catalyst was characterized by using scanning electron microscope (SEM), X-ray diffraction (XRD), infrared spectroscopy (IR) and energy-dispersive X-ray spectroscopy (EDX). The photocatalytic performance of material was evaluated by the photoredution of degradation of Amoxicillin (AMX) antibiotic under visible light. Results show that the obtained  $WO_3/Ag_3VO_4$  photocatalyst can significantly enhance photocatalytic activity in comparison with the pure  $WO_3$  and  $Ag_3VO_4$ . The enhanced photocatalytic activity of  $WO_3/Ag_3VO_4$  was predominantly attributed to the synergistic effect which increased visible-light absorption and facilitated the efficient separation of photoinduced electrons and holes.

#### Introduction

Photocatalytic degradation of antibiotics pollutants has recently become novel technology for wastewater purification [1-3]. Numerous photocatalysts including TiO<sub>2</sub>, ZnO, WO<sub>3</sub>, BiVO<sub>4</sub>, g-C<sub>3</sub>N<sub>4</sub>, FeVO<sub>4</sub>, Ag<sub>3</sub>VO<sub>4</sub>, Agl and Ag<sub>3</sub>PO<sub>4</sub> have been investigated for photocatalytic degradation of various organic pollutants [1-8]. However, the wide band gap energy (Eg  $\geq$  3,0 eV) and/or fast recombination rate of photo-excited electrons and holes are major disadvantages of these photocatalysts, leading to their low photocatalytic activity and/or the solar light could not be utilized as

excitation source for photocatalysis. An efficient photocatalyst working well under visible light for degradation of organic pollutants (pesticides, antibiotic...) should have narrow band gap energy [9]. Recently, tungsten materials, in particularly WO<sub>3</sub>, which are narrow band gap energy materials (2.8 eV), have been considered as ideal visible light-driven photocatalysts utilizing incident solar light for photocatalysis [4, 9]. However, the use of single WO<sub>3</sub> as photocatalyst for degradation of antibiotics pollutants has been limited because of the fast recombination of photo-excited electrons and holes. In addition, the photocatalyst could only utilize photo-

<sup>&</sup>lt;sup>2</sup> Faculty of Natural Sciences, Quy Nhon University, 170 An Duong Vuong, Quy Nhon City, Binh Dinh, Viet Nam

<sup>&</sup>lt;sup>3</sup> Mien Trung industry and trade college, Viet Nam, 261 Nguyen Tat Thanh, Tuy Hoa City, Phu Yen, Viet Nam

<sup>&</sup>lt;sup>4</sup>Chemical Engineering, Ho Chi Minh City University of Food Industry, 140 Le Trong Tan, Ho Chi Minh City, Viet Nam \*Email: ntplchi@hcmunre.edu.vn

excited holes in the valence band to react with H2O for production of HO\* (a strong oxidative radical degrading organic pollutants into harmless inorganic compounds such as CO<sub>2</sub> and H<sub>2</sub>O). Therefore, various have been conducted to photocatalytic activity of the WO<sub>3</sub> photocatalysts. Many previous studies have been reported that combination of WO<sub>3</sub> with another photocatalyst to establish a heterojunction system could enhance electron and hole separation efficiency as well as prevent the recombination of photo-excited electrons and holes leading to increase in its photocatalytic activity [4, 9, 10]. Due to its high stability and responsiveness to visible light, silver vanadate (Ag<sub>3</sub>VO<sub>4</sub>), another moderate band gap energy material that has attracted significant attention [11-13]. However, photocatalytic activity of the q- Aq<sub>3</sub>VO<sub>4</sub> still suffers from low conversion efficiencies due to the fast recombination of generated electrons and holes, which is usually considered as a major barrier in the single component semiconductor photocatalyst. It is still necessary to find appropriate compounds to further enhance the photocatalytic performance of Ag<sub>3</sub>VO<sub>4</sub>. The Ag<sub>3</sub>VO<sub>4</sub> modified by using other semiconductors to establish a heterojunction or direct Z scheme system have exhibited novel photocatalytic activity even under visible light [11-15].

In this paper, we intend to the development of coupling  $Ag_3VO_4$  with  $WO_3$  as a high-performance visible light photocatalyst. The well aligned straddling band structures in hybrids can restrain the photoinduced charge recombination and enhance the transfer of electron-hole pairs. The degradation of AMX as a model pollutant under visible light to evaluate photocatalytic activity of  $WO_3/Ag_3VO_4$ .

## Experimental

## Photocatalyst synthesis

To synthesize  $WO_3$  photocatalyst, sodium tungstate dihydrate ( $Na_2WO_4.2H_2O$ ) was mixed with citric acid ( $C_6H_8O_7$ ) (ratio 5:3) before dissolving in deionized water by stirring (~10 mins) to attain a clear solution, which was continuously added HCl solution (6M) to adjust pH to 1 to obtain a yellow solution. The solution was kept stirring for 30 mins before conducting hydrothermal process at 120 °C for 12 hours. The obtained product was washed by distilled water to achieve neutral pH. The cleaned product was continuously calcinated at 500 °C for 2 hours to achieve  $WO_3$ .

To synthesize Ag<sub>3</sub>VO<sub>4</sub>, 10 g AgNO<sub>3</sub> was dissolved in distilled water and stirred for 1 h at room temperature. Then, 5 M NaOH was wise-dropped to the solution to achieve pH 10 (solution A). Solution B containing 2.3 g NH<sub>4</sub>VO<sub>3</sub> dissolving in distilled water was slowly mixed and stirred with the solution A for next 1 h before centrifugating to achieve participate. Distilled water was also used to wash the participate to reach neutral pH before drying at 60 °C for 24 h to obtain Ag<sub>3</sub>VO<sub>4</sub>.

To synthesize Ag<sub>3</sub>VO<sub>4</sub>/WO<sub>3</sub>, WO<sub>3</sub> was firstly dispersed in distilled water and AgNO<sub>3</sub> solution was dropped to the WO<sub>3</sub> suspension before stirring for 1 h. Then, the solution of NaOH (5 M) was also used to adjust pH of the suspension to 10. The NH<sub>4</sub>VO<sub>3</sub> solution was wise dropped into the adjusted pH suspension, which was continuously stirred for next 7 h in dark condition before centrifugating to achieve participate. Distilled water was also used to wash the obtained participate to reach neutral pH. The washed product was dried at 60 °C for 24 h to get Ag<sub>3</sub>VO<sub>4</sub>/WO<sub>3</sub> (WA).

#### Characterization methods

The prepared materials were carefully analyzed by an X-ray diffractometer (XRD, Bruker, AXS D8) to investigate their microstructure. UV–vis absorption spectra of these photocatalysts have been conducted on a UV – Visible spectrophotometer ((UV–Vis, Shimadzu, UV–3101PC)). Infrared spectroscopy was recorded on an 760 IR spectrometer (Nicolet–USA). Photoluminescence spectra (PL) were carried out on a Fluoromax-4-type spectrophotometer (Jobin–Yvon Co, France). Energy dispersive X-ray spectroscopy was determined on a S-4800 spectrophotometer (EDX, Hitachi – Japan).

#### Photocatalysis test

Photocatalysis experiments were carried out with an aqueous solution of amoxicillin solution (20 ppm) with a dosage of 0.5 g/L. The adsorption-desorption equilibrium was archived after 150 minute stirring without irradiation. After that, a LED lamp (220 V-30 W) was turned on to provide visible light. During irradiation time, every 30 min, 5 mL sample was taken out for filtration to determine remained amoxicillin. In detail, the filtrated solution was mixed with another solution containing benzoic acid, hydrochloric acid, sodium nitride and ammonium hydroxide for complexion. The obtained product was analyzed by an UV-vis absorption spectrometer at 435 nm.

#### Results and discussion

#### Materials characterization

The crystalline structures and phases of  $Ag_3VO_4$ ,  $WO_3$  and  $WO_3/Ag_3VO_4$  photocatalysts were characterized by XRD. The XRD patterns of the obtained materials were shown in the Figure 1.

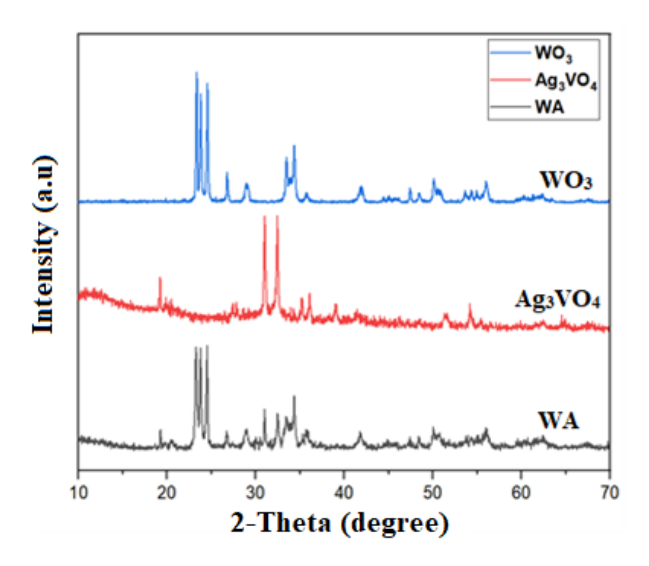


Figure 1: XRD patterns of WO<sub>3</sub>, Ag<sub>3</sub>VO<sub>4</sub> and WO<sub>3</sub>/Ag<sub>3</sub>VO<sub>4</sub>

According to the XRD pattern of the WO $_3$  indicated that observed peaks at 20 of 19.33°, 30.98°, 32.42°, 35.21°, 35.98° and 38.97° and 54.27° in the Ag3VO4 XRD pattern were indexed as (011), (–121), (121), (301), (202), (022) and (331) planes of the monoclinic typical Ag $_3$ VO $_4$  sample (JCPDS No. 43-0542) [16, 17]. Major triplet peaks of pure WO $_3$  XRD pattern exhibited major triplet peaks at 20 of 23.23°, 23.72°, and 24.41°, which corresponded to (002), (020), and (200) planes of the typical monoclinic WO $_3$  sample (JCPDS No. 43-1035) [18]. For WO $_3$ /Ag $_3$ VO $_4$  material showed two sets of characteristic peaks attributing to the WO $_3$  and Ag $_3$ VO $_4$  phases, suggesting that both components existed in the synthesized materials.

The optical properties of WO $_3$ , Ag $_3$ VO $_4$  and WO $_3$ /Ag $_3$ VO $_4$  were investigated by UV–Vis DRS. As shown in Figure 2, all samples exhibit strong absorption in the ultraviolet and part of the visible region (250–460 nm) and weak absorption in the visible region (460–800 nm). The optical absorption spectra also show that visible light absorption of the prepared WO $_3$ /Ag $_3$ VO $_4$  materials were better than that of single WO $_3$  and Ag $_3$ VO $_4$  materials.

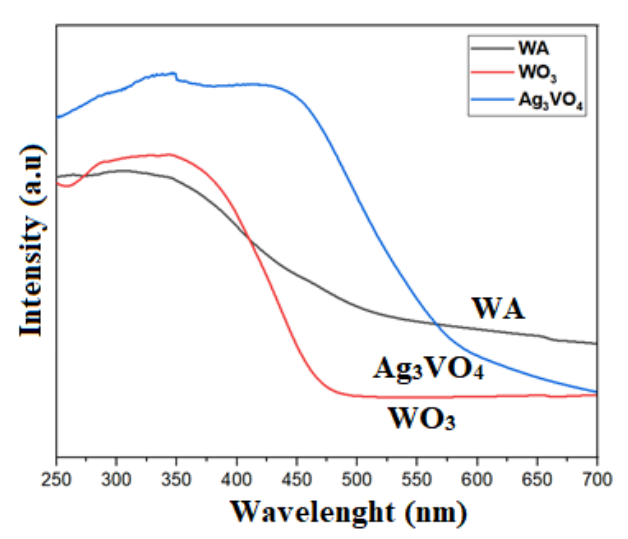


Figure 2: UV–Vis diffuse reflectance spectra of WO<sub>3</sub>,  $Ag_3VO_4$  and  $WO_3/Ag_3VO_4$ 

The calculated band-gap energies of the  $WO_3$ ,  $Ag_3VO_4$  and  $WO_3/Ag_3VO_4$  were 2.78, 2.21 and 2.74 eV, respectively (Fig. 3).

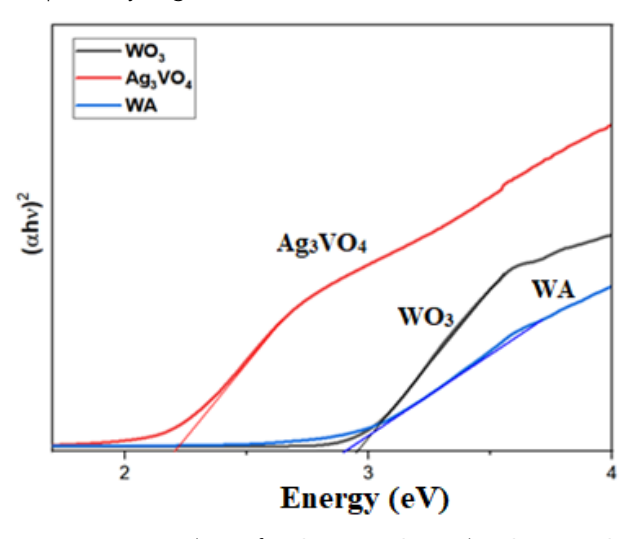


Figure 3: Tauc plots of WO<sub>3</sub>, Ag<sub>3</sub>VO<sub>4</sub> and WO<sub>3</sub>/Ag<sub>3</sub>VO<sub>4</sub>

The PL emission spectra were employed to investigate the combination and separation of the photoinduced carriers, which played a crucial role in photocatalytic reactions. The WO<sub>3</sub>, Ag<sub>3</sub>VO<sub>4</sub> and WO<sub>3</sub>/Ag<sub>3</sub>VO<sub>4</sub> PL spectra were shown in Figure 4. Pure WO<sub>3</sub> and Ag<sub>3</sub>VO<sub>4</sub> had strong PL peak intensity, the WO<sub>3</sub>/Ag<sub>3</sub>VO<sub>4</sub> heterojunction displayed lower intensity. The low PL emission intensity corresponds to the photocatalytic performance due to the recombination efficiency of the photoinduced electronhole pairs [4, 9]. Thus, the formation of heterojunction successfully solved the problem of easy recombination of photogenerated charges of single materials. The photocatalyst WO<sub>3</sub>/Ag<sub>3</sub>VO<sub>4</sub> shows luminescence emission among the prepared materials.

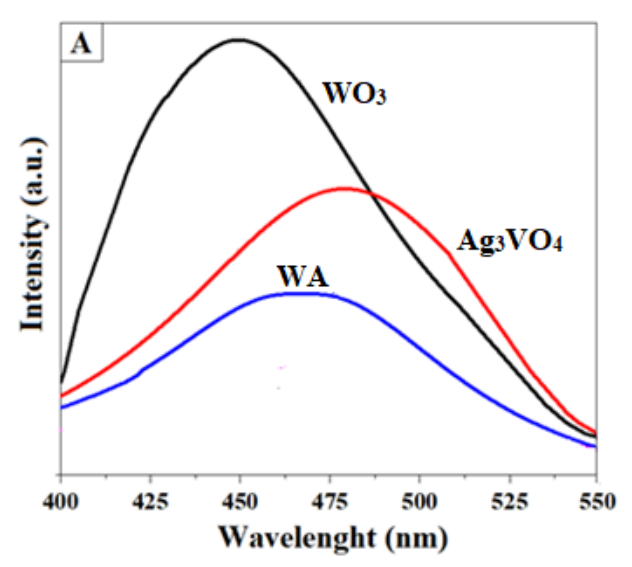


Figure 4: PL spectra of WO<sub>3</sub>, Ag<sub>3</sub>VO<sub>4</sub> and WO<sub>3</sub>/Ag<sub>3</sub>VO<sub>4</sub>

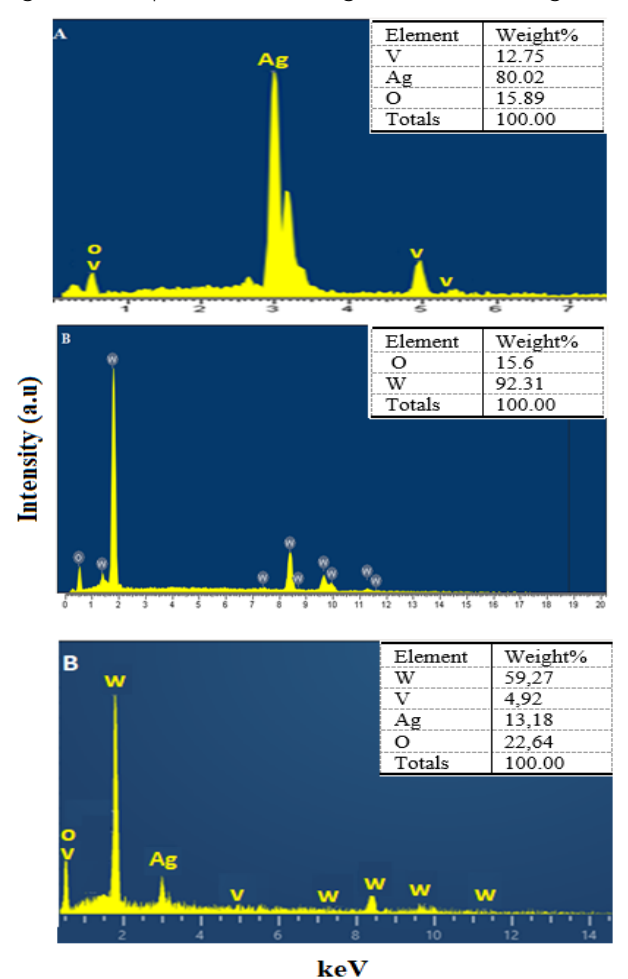


Figure 5: EDX spectra of  $Ag_3VO_4$  (a),  $WO_3$  (b) and  $WO_3/Ag_3VO_4$  (c)

Elemental composition identified by EDX is compatible with the chemical structure of  $WO_3$ ,  $Ag_3VO_4$  and  $WO_3/Ag_3VO_4$  materials. The  $WO_3$ ,  $Ag_3VO_4$  and  $WO_3/Ag_3VO_4$  EDX spectra were shown in Figure 5.

The obtained EDX spectrum (Fig 5) showed that tungsten (observed peaks at 7,43, 8,45 and 9,64 keV ), oxygen (0,51 keV), silver (3,1 keV), and vanadi (0,45 and 5,42 keV) were all detected. This indicated  $WO_3/Ag_3VO_4$  was successfully synthesized.

The molecular structure of the synthesized WO<sub>3</sub>, Ag<sub>3</sub>VO<sub>4</sub> and WO<sub>3</sub>/Ag<sub>3</sub>VO<sub>4</sub> was studied using infrared spectroscopy with a spectrometer in the range 500-4000 cm<sup>-1</sup>. The IR spectra of synthesized samples are shown in Figure 7. In the IR spectrum of Ag<sub>3</sub>VO<sub>4</sub>, the absorption peak at 745 and 868 cm<sup>-1</sup> corresponds to Ag-V and V-O in  $VO_4^{3-}$  group [12]. For the  $WO_3$ crystalline structure, the active mode vibrations of the W=O (870 cm<sup>-1</sup>), W-O (686 cm<sup>-1</sup>) bonds are owing to the octagonal structure [19]. In the binary component of WO<sub>3</sub>/Ag<sub>3</sub>VO<sub>4</sub>, two the characteristic peaks of Ag₃VO₄ at 745 and 868 cm⁻¹ were obscured after the introduction of WO<sub>3</sub> and vibrational modes at 830-852 cm<sup>-1</sup> corresponding to the W-O-W bonds is WO<sub>4</sub> or WO6. The peak at 912-938 cm-1 indicates the vibration of the W-O- and W=O bond of WO4 and WO<sub>6</sub>, indicating the coexistence of WO<sub>3</sub> and Ag<sub>3</sub>VO<sub>4</sub> semiconductors.

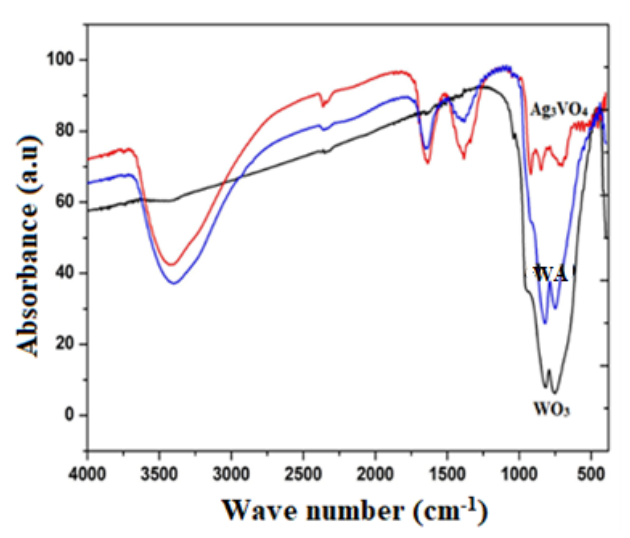


Figure 6: IR spectra of WO<sub>3</sub>, Ag<sub>3</sub>VO<sub>4</sub> and WO<sub>3</sub>/Ag<sub>3</sub>VO<sub>4</sub>

#### Photocatalytic activities

The AMX removal using WO<sub>3</sub>, Ag<sub>3</sub>VO<sub>4</sub> and WO<sub>3</sub>/Ag<sub>3</sub>VO<sub>4</sub> materials were presented in the Figure 7. The change in AMX concentration during photocatalysis under visible light was followed up by absorbances collected from UV-visible spectrophotometer at 435 nm.

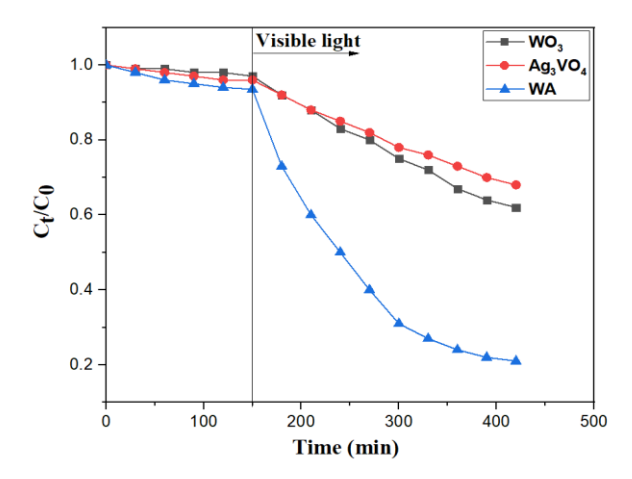


Figure 7: Conversion of AMX using WO<sub>3</sub>, Ag<sub>3</sub>VO<sub>4</sub> and WO<sub>3</sub>/Ag<sub>3</sub>VO<sub>4</sub>

Figure 7 indicates that the photocatalytic activity of WO<sub>3</sub>/Ag<sub>3</sub>VO<sub>4</sub> was better than those of WO<sub>3</sub> and Ag<sub>3</sub>VO<sub>4</sub>. After 180 min irradiating by visible light, AMX degradation of the bare WO<sub>3</sub> and Ag<sub>3</sub>VO<sub>4</sub> samples were 38.5 and 32.3%, respectively. When  $Ag_3VO_4$  was hybridized with WO<sub>3</sub> to form Ag<sub>3</sub>VO<sub>4</sub>/WO<sub>3</sub> heterojunction, its photocatalytic amoxicillin degradation was remarkedly enhanced (79,86%) as compared to these pristine WO<sub>3</sub> and Ag<sub>3</sub>VO<sub>4</sub> materials. Because of well hybridizing and matching band potentials between Ag<sub>3</sub>VO<sub>4</sub> and WO<sub>3</sub>, the photoexcited electrons at WO<sub>3</sub> conduction band would be transported from boundary to Ag<sub>3</sub>VO<sub>4</sub> valence band and combined with its holes to inhibit charge recombination in each material resulting accumulation of huge amounts of available electrons at Ag<sub>3</sub>VO<sub>4</sub> conduction and holes in WO<sub>3</sub> valence (Fig. 8). The generated electrons and holes, which were high redox potentials, effectively participated in degradation of amoxicillin.

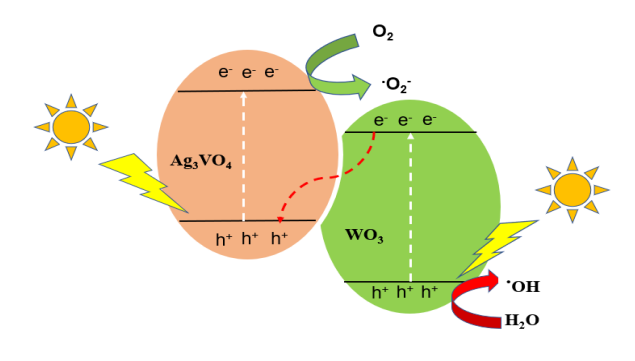


Figure 8: Amoxicillin degradation mechanism of the WO<sub>3</sub>/Aq<sub>3</sub>VO<sub>4</sub> photocatalyst.

#### Conclusion

WO<sub>3</sub>/Ag<sub>3</sub>VO<sub>4</sub> photocatalyst was synthesized and its characteristics were analyzed by XRD, SEM, IR and EDX. Photocatalyst particles were all in crystalline form. The estimated energy band gaps of the WO<sub>3</sub> and Ag<sub>3</sub>VO<sub>4</sub> were 2.78 and 2.21 eV, respectively. Thus, both WO<sub>3</sub> and Ag<sub>3</sub>VO<sub>4</sub> in WO<sub>3</sub>/Ag<sub>3</sub>VO<sub>4</sub> photocatalyst had suitable energy band gaps to absorb provided visible light for electrons jumping from VB to CB leaving holes at the VB. The WO<sub>3</sub>/Ag<sub>3</sub>VO<sub>4</sub> photocatalyst possess significantly improved visible light photocatalytic activity for AMX degradation compared with WO<sub>3</sub> and the Ag<sub>3</sub>VO<sub>4</sub>. The enhancement of photocatalytic efficiency under visible light is mainly attributed to the match of conduction and valence band levels between the WO<sub>3</sub> and Ag<sub>3</sub>VO<sub>4</sub>, which can induce the high separation of photo-generated electron-hole pairs in the heterojunction system.

## Acknowledgments

This research is funded by Ministry of Education and Training of Vietnam under grant number B2021-DQN-08.

#### References

- Y. Song, J. Gu, K. Xia, J. Yi, H. Chen, X. She, Z. Chen, C. Ding, H. Li, H. Xu, Applied Surface Science 467-468 (2019) 56-64. https://doi.org/10.1016/j.apsusc.2018.10.118
- 2. J. Zhang, Z. Ma, Materials Letters 216 (2018) 216–219. https://doi.org/10.1016/j.matlet.2018.01.035
- 3. Z. Wei, F. Liang, Y. Liu, W. Luo, J. Wang, W. Yao, Y. Zhu, Applied Catalysis B: Environmental 201 (2017) 600–606.
  - https://doi.org/10.1016/j.apcatb.2016.09.003
- Y. Yang, B. Liu, J. Xu, Q. Wang, X. Wang, G. Lv, J. Zhou, ACS Omega 7 (2022) 6035–6045. https://doi.org/10.1021/acsomega.1c06377
- V. X Doorslaer, P. M. Heynderickx, K. Demeestere, K. Debevere, Van H. Langenhove, J. Dewulf, Applied Catalysis B: Environmental (2012) 150-156. https://doi.org/10.1016/j.apcatb.2011.09.029
- R. Huo, X. L. Yang, Y. Q. Liu, Y. H. Xu, Materials research bulletin 88 (2017) 56-61. https://doi.org/10.1016/j.materresbull.2016.12.012
- 7. S. Yan, Z. Li, Z. Zou, Langmuir 25 (2009) 10397-10401. https://doi.org/10.1021/la900923z
- Zhang, Y. Jiang, Journal of Solid State Chemistry
  268 (2018) 83-93. https://doi.org/10.51316/jca.2022.053

- https://doi.org/10.1016/j.jssc.2018.07.031
- M. Zhou, T. Tian, H. Zhonghua Wang, C. Ren, L. Zhou, Y-W Lin, L.Dou, ACS Omega 6 (2021) 26439–26453. https://doi.org/10.1021/acsomega.1c03694
- 10. Y. Wang, D. Chen, Y. Hu, L. Qin, J. Liang, X. Sun, Y. Huang, Sustainable Energy Fuels 4 (2020) 1681-1692.
  - https://doi.org/10.1039/C9SE01158G
- M. Tang, Y. Ao, C. Wang, P. Wang, Applied Catalysis B: Environmental 268 (2020) 118395. https://doi.org/10.1016/j.apcatb.2019.118395
- K. Polat, M. Yurdakoc, Water Air Soil Pollution, 10 (2018) 229-331. https://doi.org/10.1007/s11270-018-3959-y
- W. Zhao, Y. Feng, H. B. Huang, P. H. Zhou, J. Li, L. Zhang, B. L. Dai, J. M. Xu, F. X. Zhu, N. Sheng, D. Y. C. Leung, Applied Catalysis B: Environmental 245 (2019)
  448-458. https://doi.org/10.1016/j.apcatb.2019.01.001

- M. Yan, Y. Wu, F. Zhu, Y. Hua, W. Shi, Physical Chemistry Chemical Physics, 18 (2016) 3308-3315. https://doi.org/10.1039/C5CP05599G
- T. Zhu, Y. Song, H. Ji, Y. Xu, Y. Song, J. Xia, H. Li, Chemical Engineering Journal 271 (2015) 96-105. https://doi.org/10.1016/j.cej.2015.02.018
- Z. Liu, L. Chen, C. Piao, J. Tang, Y. Liu, Y. Lin, D. Fang, J. Wang, Applied Catalysis A: General 623 (2021) 118295.
  https://doi.org/10.1016/j.apcata.2021.118295
- L. Jing, Y. Xu, C. Qin, J. Liu, S. Huang, M. He, H. Xu, H. Li, Materials research bulletin 95 (2017) 607–615. https://doi.org/10.1016/j.materresbull.2017.06.003
- 18. A. Dehdar, G. Asgari, M. Leili, T. Madrakian, A. Seid-mohammadi, Journal of Environment Management 297 (2021) 113338.
- P.S. Kolhe, P.S. Shirke, N. Maiti, M.A. More, K.M. Sonawane, Journal of Inorganic and Organometallic Polymers and Materials 29 (2018) 41-48. https://doi.org/10.1007/s10904-018-0962-0